

A²P-MANN: Adaptive Attention Inference Hops Pruned Memory-Augmented Neural Networks

Mohsen Ahmadzadeh¹, Mehdi Kamal¹, Ali Afzali-Kusha¹, and Massoud Pedram²

¹School of Electrical and Computer Engineering, College of Engineering, University of Tehran, Iran

²Department of Electrical Engineering, University of Southern California, USA

{mohsen.ahmadzadeh, mehdikamal, afzali}@ut.ac.ir, pedram@usc.edu

Abstract—In this work, to limit the number of required attention inference hops in memory-augmented neural networks, we propose an online adaptive approach called A²P-MANN. By exploiting a small neural network classifier, an adequate number of attention inference hops for the input query is determined. The technique results in elimination of a large number of unnecessary computations in extracting the correct answer. In addition, to further lower computations in A²P-MANN, we suggest pruning weights of the final FC (fully-connected) layers. To this end, two pruning approaches, one with negligible accuracy loss and the other with controllable loss on the final accuracy, are developed. The efficacy of the technique is assessed by using the twenty question-answering (QA) tasks of bAbI dataset. The analytical assessment reveals, on average, more than 42% fewer computations compared to the baseline MANN at the cost of less than 1% accuracy loss. In addition, when used along with the previously published zero-skipping technique, a computation count reduction of up to 68% is achieved. Finally, when the proposed approach (without zero-skipping) is implemented on the CPU and GPU platforms, up to 43% runtime reduction is achieved.

Keywords—Memory-Augmented Neural Networks, Computation Reduction, Latency Reduction, Dynamic Reconfiguration, Pruned Neural Networks, Approximate Computing.

I. INTRODUCTION

Deep Neural Networks (DNNs) are used widely for different applications including image and text classification, as well as speech recognition and other natural language processing (NLP) tasks. As their size (depth and width) grow so as to achieve higher output accuracies, these networks consume more energy due to higher computational complexity along with more memory accesses [1]. A variety of techniques have been proposed to reduce the computational costs, and in turn, the energy consumption of DNNs. Examples of the techniques include weight compression and quantization [2], pruning the weights and connections [3, 4], runtime configurable designs [5, 6], and approximate computing [7].

An emerging type of neural networks is the Memory Augmented Neural Network (MANN), which is based on recurrent neural networks (RNNs). MANNs are highly effective in processing long-term dependent data. Examples of this type of network are those developed by Facebook [8, 9], Neural Turing Machines (NTM) [10], and Differentiable Neural Computers (DNC) [11]. MANNs are equipped with a differentiable associative memory which is used as a scratchpad or working memory to store previous context and input sequences (e.g., sentences of a story) to increase the learning and reasoning ability of the models [12]. This powerful reasoning ability has made the utilization of MANNs common in many application fields including simple dialog systems, document reading, and question

answering (QA) tasks [8, 13–15]. More specifically, in QA tasks, MANN, first, receives a set of sentences describing a story and the network stores them in its augmented memory. Next, a question is passed to the network which is about the information presented in the story where MANN performs several iterations over an attention-based inference mechanism (called attention inference in the rest of paper) to find the correlation between each story sentence and the question. At the end, this information is employed by a Fully Connected (FC) layer (called the output layer) to generate the answer.

To perform their tasks, different kinds of complex and intensive computations (e.g., dot product calculations) should be performed [16]. The same operations are performed in each layer (a.k.a., hop) of the MANN. Taking multiple hops to greedily attend to different facts is necessary to achieve a high accuracy [8]. The general structure of MANNs for QA tasks is shown in Fig. 1.

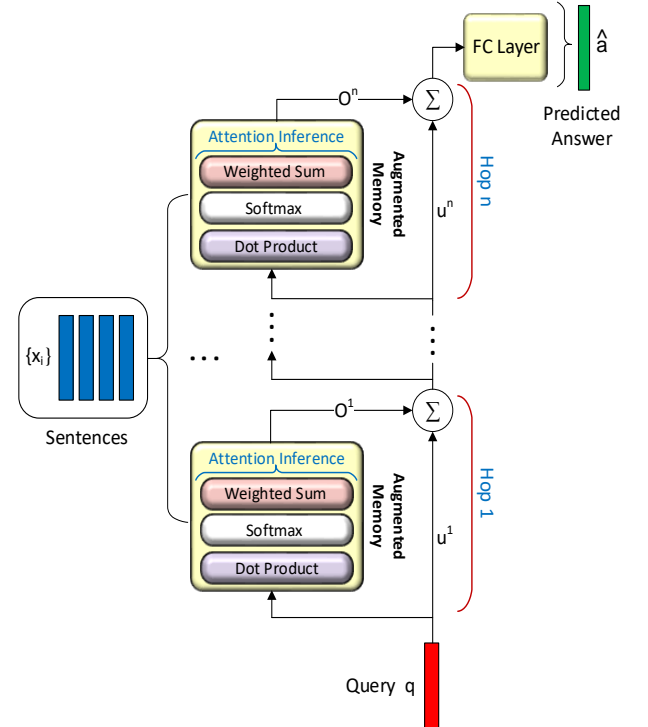


Figure 1. The general structure of MANNs for QA tasks.

When dealing with real-world problems, these networks require more electrical energy and memory space than most mobile devices can provide [17, 18]. For example, thousands to millions of memory locations may be required for the operations of the network. Hence, the latency and energy consumption of these networks, especially, in embedded systems, may be problematic. On other hand, in the case of IoT applications, the computations may be performed on

remote servers. This is feasible only when a communication network is available and also results in low performance [18]. For the above reasons, any effort to reduce the computation burden and energy consumption of MANNs with negligible accuracy reduction is highly desirable.

Since MANN is a recently introduced neural network architecture, the number of works published in the literature focusing, specifically, on reducing the computational complexity of MANNs is limited. To speed up the inference and reduce the operation time of the output layer of MANNs, an inference thresholding method which is a data-based method for maximum inner-product search (MIPS) has been presented in [18]. To reduce the memory bandwidth consumption, reference [16] presented a column-based algorithm with streaming for optimizing the softmax and weighted sum operations, which minimizes the size of data spills and hides most of the off-chip memory accessing overhead. Second, to decrease the high computational overhead, reference [16] introduced a zero-skipping optimization to bypass a large amount of output computation. These works are reviewed in more detail in Section II.

In this work, we present a runtime dynamic technique which adaptively sets the required amount of attention inference hops of MANNs for the input queries in QA applications. The technique employs a small neural network classifier to determine the difficulty level of the input query (*Easy* or *Hard*), based on which the required number of hops to find the final answer is decided. Since the decision is made based on the output of the first hop, a considerable amount of computation may be avoided. To further reduce the energy consumption, we present two approaches for pruning the FC layer of the MANN. The efficacy of the proposed adaptive attention inference hops pruned MANN (called A²P-MANN) is evaluated in 20 QA tasks of the Facebook bAbI dataset [19].

The remainder of the paper is organized as follows. In Section II, the related work is reviewed. This is followed by a discussion of the structure of MANNs as well as their computational complexity in Section III. We present details of the proposed A²P-MANN inference method in Section IV. Simulation results for the efficacy evaluation of the proposed inference method are given in Section V, and finally, the paper is concluded in Section VI.

II. RELATED PRIOR WORK

A wide range of approaches to improve the energy and computation efficiency in conventional DNNs (CNNs) have been pursued (see, *e.g.*, [2]–[7]). Interestingly, the intrinsic fault-tolerance feature of NNs allows using approximation methods to optimize energy efficiency with insignificant accuracy degradation [20, 21]. As an example, to reduce the computational complexity, an approximation method based on removing less critical nodes of a given neural network was proposed in [7]. Also, similar pruning techniques have been employed for resource constrained environments like embedded systems [4, 22, 23]. The amount of fault tolerance and resilience varies from one model/structure to another [24]. The efficacy of using approximation on MANNs has been investigated by some prior works (see, *e.g.*, [16], [18]). In [16], three optimization methods to reduce the computational complexity of MANNs were suggested. The first one which was suggested to reduce the required memory bandwidth, was a column-based algorithm that minimized the

size of data spills and eliminated most of the off-chip memory access overhead. To bypass a large amount of computations in the weighted sum step during the attention inference hops, zero-skipping optimization was proposed as the next technique. In this technique, by considering a zero-skipping threshold (θ_{zs}), the weighted some operations corresponding to the values less than θ_{zs} in the probability attention vectors (p^a) were omitted. Since the query is only related to a few sentences in the story, a majority of these weighted some operations in the output memory representation step could be skipped using this approach [16]. Finally, an embedding cache was suggested to efficiently cache the embedding matrix.

In [18], a MANN hardware accelerator was implemented as a dataflow architecture (DFA) where fine-grained parallelism was invoked in each layer. Moreover, to minimize the output calculations, an inference thresholding technique along with an index ordering method were proposed. A differentiable memory has soft read/write operations addressing all the memory slots through an attention mechanism. It differs from conventional memories where read/write operations are performed only on specific addresses. Realizing differentiable memory operations have created new challenges in the design of hardware architectures for MANNs. In [25], an in-memory computing primitive as the basic element used to accelerate the differentiable memory operations of MANNs in SRAMs, was proposed. The authors suggested a 9T SRAM macro (obviously different from cell) capable of performing both Hamming similarity and dot products (used in soft read/write and addressing mechanisms in MANNs).

In [17], a memory-centric design that focused on maximizing performance in an extremely low FLOPS/Byte context (called Manna) was suggested. This architecture was designed for DeepMind’s Neural Turing Machine (NTM) [10], which is another variant of MANNs, while we have focused on end-to-end memory networks (MemN2N) [8]. Note that these prior works have offered special hardware architectures for MANNs. In this work, however, we propose A²P-MANN technique which is independent from the hardware platform and could be executed on any of these accelerators.

Some runtime configurable designs that give the ability to trade-off accuracy and power during inference have been proposed in the literature [5, 6, 26]. In [5], a Big/Little scheme was proposed for efficient inference. The big DNN (which has more layers) is executed only after the result of the little DNN (with fewer layers) is considered to be not accurate according to a score margin defined for the output softmax. To improve the efficiency of CNNs in computation-constrained environments and time-constrained environments, multi-scale dense networks were suggested in [26]. For the former constraint, multiple classifiers with varying resource demands, which can be used as adaptive early-exits in the networks during test time, are trained. In the case of the latter constraint, the network prediction at any time can be facilitated. A method of conditionally activating the deeper layers of CNNs was suggested in [27]. In this method, an additional linear network of output neurons was cascaded to each convolutional layer. Using an activation module on the output of each linear network determined whether the classification can be terminated at the current stage or not.

III. MEMORY AUGMENTED NEURAL NETWORKS

A. Notation

The following notation is adopted in this paper:

- BOLDFACE UPPER CASE to denote matrices.
- Boldface lower case to denote vectors.
- Non-boldface lower case for scalars.
- The “.” sign is used for the dot product.
- No signs are used for the scalar product or matrix-vector multiplication.

B. Basic Structure of MANN

MANNs are efficient in solving QA tasks (e.g., bAbI QA tasks) in which the system provides answers to the questions about a series of events (e.g., a story) [8]. A MANN takes a discrete set of inputs s_1, \dots, s_n which are to be stored in the memory, a query q , and outputs an answer a . Each of the s_i , q , and a contains symbols coming from a dictionary with V words. The model writes all s_i to the memory up to a fixed buffer size, and then finds a continuous representation for the s and q . The continuous representation is then processed via multiple hops to output a [8]. An example of these tasks is shown in Fig. 2. These networks have three main computation phases comprising embedding, attention inference, and output generation.

s1:	Mary picked up the apple.
s2:	John went to the office.
s3:	Mary journeyed to the garden.
s4:	Mary went to the bedroom.
q:	Where was the apple before the bedroom?
a:	Garden.

Figure 2. An example of story, question, and answer

In the embedding phase, embedding matrices A and C (which elements are obtained in the training phase) of size $d \times V$ (where d is the embedding dimension and V is the number of words in the dictionary), are used in a bag-of-words (BoW) approach to embed the story sentences into the input and output memory spaces (M^{IN} and M^{OUT} with the size of $d \times n_s$), where n_s denotes the number of sentences in the story. Let n_w denote the number of words per sentence. If the number of story sentences (words of a sentence) is less than n_s (n_w), the story (sentence) is enlarged to n_s sentences (n_w words) by zero padding. Thus, for each story, $n_s \times n_w$ words are considered in MANNs.

In the embedding phase, first, each input story is represented by a matrix of size $n_s \times n_w$, which elements are obtained by mapping words of the sentences to their corresponding integer values based on the given dictionary. Next, for each sentence, elements of its corresponding row are used as the row indices of the embedding matrix A . The rows of A are chosen to represent each word as a vector of size $1 \times d$. This leads to representing each sentence of size $n_w \times 1$ by a matrix of size $n_w \times d$. To preserve the order of the words in each sentence, and improve the output accuracy, an element-wise product of a positional encoding (PE) matrix (of size $n_w \times d$) and the matrix representation of each sentence is performed (details about PE are provided in [8]). Next, elements of the resulting matrix for each sentence are summed along the column direction and transposed, giving rise to the representation of each sentence by a column vector of size $d \times 1$ (called “internal state” of each sentence). These vectors are then stored in M^{IN} to form matrices of size $d \times n_s$

for each story. A similar approach is employed to embed the input story in M^{OUT} by using the embedding matrix C . Also, the query (of length n_w words) is embedded by using another embedding matrix B (of size $d \times V$). The output of this phase is the internal state of the query denoted by column vector u (or u^I) of size $d \times 1$.

The attention inference phase consists of four parts: inner product, softmax attention, weighted sum, and output-key sum. First, the match between u and each input memory vector (i.e., the internal state of each sentence in M^{IN} which is a column vector of size $d \times 1$) is obtained by computing the vector-matrix dot product

$$k = u^T \cdot M^{IN} \quad (1)$$

where u^T denotes transpose of u and k is of size $1 \times n_s$. Applying a Softmax operator to the resulting vector gives the probability-attention vector (p^a) over the inputs (i.e., $p^a = \text{Softmax}(k)$). An output vector o (of size $d \times 1$) is obtained by calculating the sum over the output memory vectors (the internal state of each sentence in M^{OUT} which is a column vector of size $d \times 1$ denoted by m_i^{out}) weighted by the corresponding probability value (p_i^a which is a scalar)

$$o = \sum_i p_i^a m_i^{out} \quad (2)$$

The sum of the output vector o and the query key u ($u^{out} = o + u$) is then presented as the output-key (u^{out}) of this phase. In the output generation stage, the network has a fully connected (FC) linear layer in which the final weight matrix W (of size $d \times V$) is multiplied by the output key u^{out} to produce the final answer. Thus, the final output (\hat{a}) is obtained from

$$\hat{a} = \text{Softmax}(W^T u^{out}) \quad (3)$$

This means that, to obtain the final output in the training phase, the softmax operation is necessary whereas it may be omitted in the inference phase [18]. This step, independent from the hop counts, is executed once as the last step.

To improve the accuracy, MANNs use multiple hop operations [8]. During each of these hops, MANN has a different probability-attention vector over the sentences (facts). Thus, the network concentration is directed towards different facts in each hop that eventually leads to the true output answer [8]. The computations that are performed in each hop depend either on the employed weight tying method or the application type [8, 16, 28]. In this work, for making the MANNs, we employ the adjacent weight tying approach [8]. In this approach, the story sentences are embedded in the input/output memory cells using different embedding matrices in each hop (a similar method is used in the Hop-specific approach of reference [29]). This means that each hop contains (assuming the adjacent weight tying approach of [8]) two story embeddings and an attention-based inference. The first hop has also a query embedding. Based on the provided explanations, the general structure of a three-layer MANN, which is used in this work is shown in Fig. 3. The structure is based on the MANN architecture described in [8].

C. Computational Complexity

The computational complexity of MANN could be described based on the number of the required floating-point operations (FLOPs). The number of FLOPs for each operation in MANN is shown in Table 1 where the addition

Table 1. Number of floating-point operations (FLOPs) for each operation in MANN structure.

Operation	FLOPs	Operation	FLOPs
Query/PE embedding	$(2 \times n_w - 1) \times d$	Weighted Sum	$(2 \times n_s - 1) \times d$
Story/PE embedding	$n_s \times (2 \times n_w - 1) \times d$	Output Key Sum	d
Story/Query Inner Product	$n_s \times (2 \times d - 1)$	FC layer	$V \times (2 \times d - 1)$
Softmax attention	$n_s \times 13 - 1$		

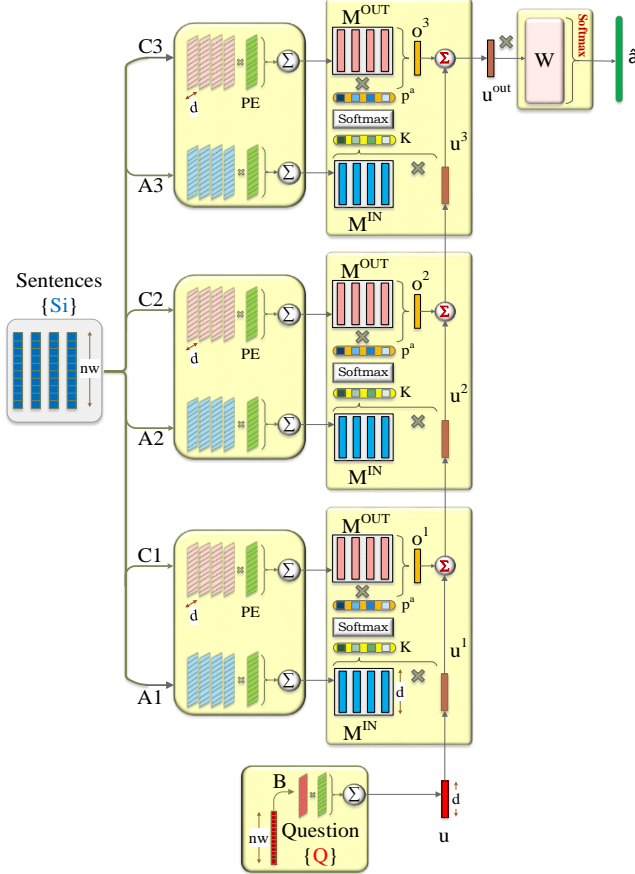


Figure 3. Computational steps of a 3-hop MANN.

and multiplication operations are counted as 1 FLOP, while each division and exponential are considered as 4 and 8 FLOPs, respectively [30]. During the inference phase in which the input and output memories are usually available, the story sentences are previously embedded to their internal states. Thus, the user only submits question sentences to be answered based on the provided database (*i.e.*, story sentences) [16]. Nevertheless, for interactive applications, the user can provide both the database and the query to be answered [16]. Since, in the latter case, the database is changed for each question, its computational complexity would be significantly larger than that of the former one. We refer to the applications in former (latter) approach as pre-embedded (interactive) applications. Now, using the figures and the table, the computational complexity (CC) of one hop for pre-embedded ($CC_{H,E}$) and interactive ($CC_{H,I}$) applications may be obtained by

$$CC_{H,E} = n_s \times (4 \times d + 12) - 1 \quad (4)$$

$$CC_{H,I} = n_s \times [(4 \times n_w + 2) \times d + 12] - 1$$

Also, the computational complexity of a three-hop MANN (considering the final FC layer) in the cases of the pre-embedded (CC_E) and interactive (CC_I) applications are also determined from

$$\begin{aligned} CC_E &= (2 \times n_w - 1) \times d + 3 \times CC_{H,E} \\ &\quad + V \times (2 \times d - 1) \\ CC_I &= (2 \times n_w - 1) \times d + 3 \times CC_{H,I} \\ &\quad + V \times (2 \times d - 1) \end{aligned} \quad (5)$$

IV. PROPOSED A²P-MANN

A. Motivation

Using multiple computational steps, also called hops or layers, is crucial for improving the average accuracy of MANNs [8]. Very often, three or more hops are utilized. In our study, we observe that a significant portion of the queries can be answered with only one hop not requiring more computation for reaching the correct answer. This motivated us to develop an online mechanism required to identify these inputs (queries), denoted as Easy Input queries (Q_E), for bypassing the computations of the additional hops at runtime. Obviously, this will result in lower computations and, in turn, less energy consumption per inference. In addition, as mentioned before, the final answer is determined by using a FC layer. Our observation shows that many weights of this layer do not have a great impact on the final result of the MANN. Therefore, pruning this layer leads to a lower latency as well as lower memory usage for storing the weights without sacrificing the output accuracy. Based on these observations, we present the A²P-MANN structure.

B. Proposed Structure Overview

We suggest two methods for the computation reduction of the conventional MANNs. The methods are (i) employing input classifier network (ICN) at the output of the first hop and (ii) pruning the FC layers. In this work, the baseline network is a jointly trained 3-layer version of MANNs proposed in [8]. In A²P-MANN, weights of the baseline MANN are exploited in shared components. ICN, which is a small network formed by two linear layers, is responsible for classifying the output key of the first hop (u^2) to *Easy* and *Hard*. During the inference step, if the ICN identifies the input query as Easy (Q_E), only one hop is computed, while for Hard-identified input queries (Q_H), all the three hops are applied. For pruning the FC layers, we suggest two approaches to eliminate some rows of the weight matrix of the FC layers (see below). Finally, to further reduce computations in A²P-MANN, one may use the zero-skipping approach suggested in [16]. The general structure of the proposed A²P-MANN is depicted in Fig. 4. In the following subsections, the details of the proposed technique are discussed.

C. Input Classifier Network (ICN)

When ICN determines that the input query is an easy one, the output of the first hop, u^2 , is passed to a FC layer (denoted as FC_E) trained to classify the easy queries. If ICN finds the input query as a hard one, it passes u^2 to the second

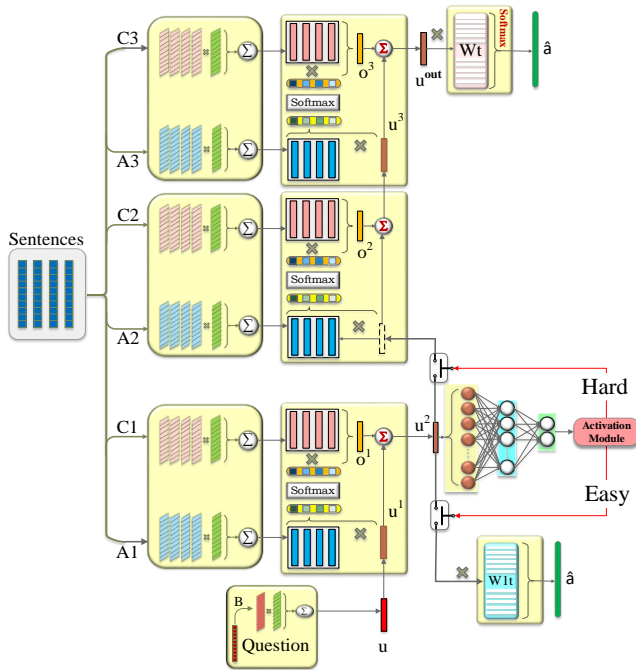


Figure 4. The general structure of the proposed A²P-MANN

hop where after computing the remaining hops, the response to the input query is obtained at the output of the FC layer (denoted as FC_H). The FC layer uses the output of the final (third hop in this work) hop. In the proposed approach, FC_H is the same FC layer as that of the baseline MANN.

FC_E layer: The architecture of FC_E is the same as the FC_H, while the weights of the FC_E (W_E as the corresponding weight matrix) are trained based on the output of the first hop. In this work, we considered the weights of the FC_H as the initial weights for the training of FC_E. In the training phase, FC_E is trained while the pretrained embedding matrices are frozen. This layer is trained by the all the input queries from the training set of the considered dataset. Also, the FC_E layer is trained before training the ICN.

ICN Labels: Because the ICN’s goal is to classify the queries into easy and hard, for each query of the considered dataset, it should generate a label. For this, each story-query input is fed into an evaluation process using both 1-hop and 3-hop states of the network. In this process, when the FC_E layer provides correct response, label *Easy* is considered for that input query. If the FC_E output is not correct and FC_H provides the correct answer, *Hard* is assigned as the label for the input query. Note that if neither of the states could predict the true label for an input, we assign label *Easy* to gain more computation reduction without sacrificing the output accuracy.

ICN Architecture: This network should be designed based on the considered dataset. In this work, we designed ICN based on 20 tasks of bAbI, which is a commonly used dataset for MANNs (see, *e.g.*, [8, 16–18, 25, 29]). Our investigation shows that implementing ICN using small linear layers can provide an acceptable accuracy. In this work, a two-linear-layer network achieves up to 86% accuracy in classifying input queries. The first layer of this network transfers the input (u^2) of size d , which is 40 in our study, to a hidden layer of 32 neurons. Notice that ReLU is used as the activation function of the hidden layer neurons. The 32

neuron outputs are then transferred to the output layer of 2 neurons for labeling the tasks as *Easy* or *Hard*.

Using an Activation Module: Because the accuracy of ICN may not reach 100%, having false-positive inputs (*Hard* inputs that are identified as *Easy* by ICN) is inevitable. These incorrect classifications will lead to A²P-MANN accuracy degradation. Using the activation module of [27] at the output layer of the ICN can be helpful. The said module utilizes the confidence value (probability value, z) at the output neuron as well as a predefined confidence value threshold to decide whether the input query should be classified as *Easy* or *Hard*. More specifically, the activation module is an “if statement” which compares the maximum of the two outputs of ICN (logits/probabilities) with a threshold. When the maximum value (*i.e.*, the confidence value) belongs to the *Easy* output and is larger than the threshold, the implication is that the input is easy and invokes FC_E to compute the answer after the first hop. If the confidence value is less than the threshold, the answer is determined by performing the computations for all the hops. Utilizing this module has the drawback of increasing the number of false-negative inputs (*Easy* inputs that are identified as *Hard* by ICN) and consequently, abandoning some of the computational savings. Fortunately, this increase does not deteriorate the accuracy. Based on the above explanation, the output of ICN should pass through a softmax layer before entering the activation module.

D. Pruning Weight Matrices of FC layers

Owing to the large dimension of MANN output (which is the number of words in the dictionary), fine-grained parallelism is a challenge for the computations in the last FC layer. Methods such as serializing some dot products by defining an inference thresholding method and therefore ignoring some dot products of this layer have been suggested in literature (i.e., [18]).

Our investigation shows that for the bAbI dataset, more than 65% of the words in the dictionary are not among the training labels, and thus, are never the answer to any question in the training data. In other words, the memory network architecture is not trained to pick up the answer among them. This is a direct consequence of the fact that a limited number of words from the dictionary are used as the answers for the questions. Hence, we suggest that the corresponding rows for those words (called *unused* rows) in the final weight matrices (W and W_E) be eliminated in the inference phase. This should not have any adverse effects on the final accuracy. In addition, we suggest to prune *unimportant* rows from the final weight matrices. This pruning leads to a very small accuracy loss. Setting a pruning threshold, symbolized by θ_p , unimportant rows are defined as the ones in which a notable number of weights, denoted by N_p , have absolute values less than θ_p . By applying these two pruning approaches, a significant portion of the output calculation is eliminated and application of fine-grained parallelism to the operations of the output layer may become possible. In some cases, the two proposed pruning approaches may suggest pruning of the same row(s), depending on the considered values of θ_p and N_p , which are functions of the maximum tolerable accuracy loss. It should be noted that considering larger (smaller) values for N_p (θ_p) would result in less

accuracy loss. Note that, in this work, we use the same values of θ_p and N_p for pruning in both cases of FC_H and FC_E .

It is worth mentioning that while *unused* and *unimportant* rows are useless in the FC layers, they should be considered in the attention inference hops as explained next. During the output generation step (FC layers), the network finds some type of similarity between each row (corresponding to a word) and the output key u^{out} . Thus, in this way, the word with the maximum similarity will be the maximum logit or the answer. The corresponding word indices of the rows that we prune in the final weight matrices of the FC layer are not among the training labels. Therefore, during the training phase, the weights in those rows in W (and W_E) have small absolute values leading to the least similarity with the output key of the final hop. Hence, they yield the lowest logits making them unimportant in the FC layer. These rows, however, are important for the embedding and attention-based inference step, and hence pruning them in the embedding matrices will lead to some accuracy degradation. This is because when producing the attention vector, the network finds the degree of similarity between each sentence of the story and the question making every word important in those steps.

E. Computational Complexity of A²P-MANN

Based on the provided details of the proposed A²P-MANN, the computational complexity (in FLOPs) of this structure for the two cases of the pre-embedded and interactive applications could be obtained, respectively, using

$$\begin{aligned} CC_E &= \zeta_E \times 2 \times CC_{H,E} + P_R \times [V \times (2 \times d - 1)] \\ &\quad - [2 \times L_1 \times (d + 2) + 25] \\ CC_I &= \zeta_E \times 2 \times CC_{H,I} + P_R \times [V \times (2 \times d - 1)] \\ &\quad - [2 \times L_1 \times (d + 2) + 25] \end{aligned} \quad (6)$$

where the parameter ζ_E is the probability of an input query to be classified as an *Easy* input by ICN. Recall that V denotes the number of words in the dictionary. P_R is the ratio of the pruned rows to total number of rows in the final FC layers (*i.e.*, FC_H and FC_E). The last terms of the provided formulas show the overhead of the considered ICN network, where L_1 is the number of the ICN hidden layer neurons. Obviously, when an ICN with more hidden layers is employed, the considered ICN overhead has to be modified.

By applying the zero-skipping approach to A²P-MANN, more computation will be eliminated. In this case, the computational complexity of the A²P-MANN may be determined as follows

$$\begin{aligned} CC_E &= \zeta_E \times 2 \times CC_{H,E} + P_R \times [V \times (2 \times d - 1)] \\ &\quad + ((\zeta_E \times \Psi_E + (1 - \zeta_E) \times 3 \times \Psi_H) \times [(2 \times n_s - 1) \times d]) \\ &\quad - [2 \times L_1 \times (d + 2) + 25] \\ CC_I &= \zeta_E \times 2 \times CC_{H,I} + P_R \times [V \times (2 \times d - 1)] \\ &\quad + ((\zeta_E \times \Psi_E + (1 - \zeta_E) \times 3 \times \Psi_H) \times [d \times (n_s \times (2 \times n_w + 1) - 1)]) \\ &\quad - [2 \times L_1 \times (d + 2) + 25] \end{aligned} \quad (7)$$

where, Ψ_E (Ψ_H) is the average ratio of the number of skipped values to n_s (the total number of values in the probability-attention vector) for *Easy* (*Hard*) input queries in the A²P-MANN.

V. RESULTS AND DISCUSSION

A. Simulation Setup

The efficacy of A²P-MANN inference technique was assessed using 20 QA tasks of the bAbI question and answer dataset [19]. The testset consisted of 20,000 samples where each involved a story (n_s sentences), a query, and a label (answer) as shown in Fig. 2. Each task had 1,000 samples implying 20 tasks for the samples. As stated previously, the baseline network was a jointly trained 3-layer version of MANN with adjacent weight tying and positional encoding (PE) multiplications [8]. The parameters d (embedding size), n_s (number of sentences), and V (vocabulary size in dictionary) was, 40, 50 and 174, respectively.

Also, the proposed ICN was consisted of two linear layers with 32 and 2 neurons. It was trained jointly on all tasks where a weighted cross entropy loss function was used. Also, the Adam optimizer with a learning rate of 0.01 was invoked in the study. Since the quality of the MANN answers strongly depends on hyperparameters tuning in its training process, the training quality of ICN is dependent on the (pre)trained embedding matrices [8]. This had us to utilize the joint version of the TensorFlow source-code of [31] for determining the pretrained matrices while implementing the networks by PyTorch [32]. In this work, the bAbI dataset with 1k training problems per task for training of the ICN was used.

To improve the ICN accuracy, confidence-value thresholds under two cases of a global threshold for all tasks (*i.e.*, $z_G = 0.6$) and per-task thresholds (*i.e.*, $z_{pt,i}$ where i refers to the i^{th} task) were considered. Table 2 reports the z_{pt} for each task of the bAbI dataset. For some tasks (*e.g.*, the first task), since the activation module did not improve the accuracy of ICN, it was omitted from ICN, and hence, confidence thresholds have not been reported for them. These thresholds were found empirically using the training dataset and depended on both pre-trained embedding matrices and ICN trained layers.

We have suggested two pruning approaches for the final FC layers including eliminating the *unused* and *unimportant*

Table 2. The considered per-task confidence value thresholds (z_{pt}) for the trained ICN.

Task	P	Task	P	Task	P	Task	P
2*	0.52	8	0.68	12	0.8	18	0.99
3	0.8	9	0.85	14	0.84	19	0.59
6	0.95	10	0.99	15	0.67		

* The tasks that are not mentioned did not need an activation module in the ICN.

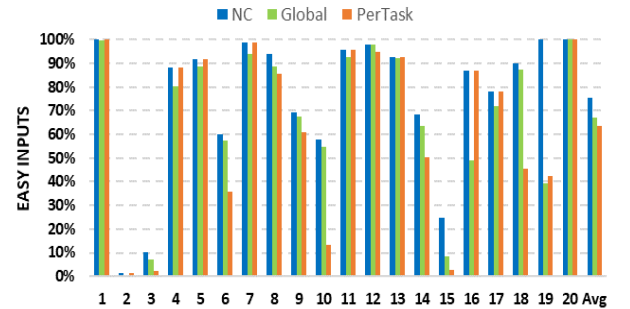


Figure 5. Percentage of Easy-classified inputs using ICN under three considered scenarios for the confidence value.

Table 3. The minimum and maximum False Positive and False Negative metrics of ICN in bAbI tasks for three considered scenarios.

	Considered Scenario	Minimum (corresponding task(s))	Maximum (corresponding task(s))	Average
False Positive	NC	0% (20)	13.5% (16)	4.78%
	Global	0% (20)	8.7% (17)	3.73%
	PerTask	0% (20)	13.5% (16)	3.19%
False Negative	NC	0% (1,19,20)	42.8% (3)	9.21%
	Global	0% (20)	53.7% (19)	15.27%
	PerTask	0% (1,20)	50.9% (19)	17.81%

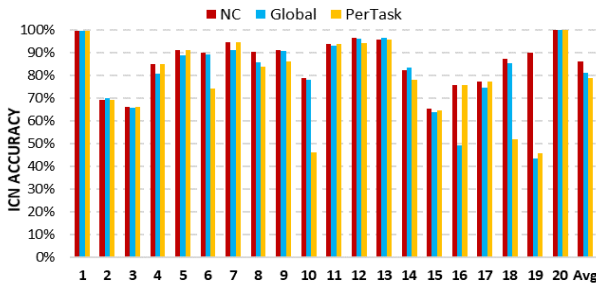


Figure 6. Accuracy of ICN for the considered scenarios.

rows. For the latter, the values of 0.1 and 13 for the parameters θ_p and N_p , respectively, were considered which led to no accuracy degradation. Also, more than 90% of the selected *unimportant* rows were the *unused* rows. Finally, by increasing θ_p (and/or decreasing N_p) more rows are omitted, degrading the accuracy.

B. Results and Discussion

ICN efficacy: The percentages of input queries, in each task, detected as *Easy* by ICN for three confidence threshold scenarios are illustrated in Fig. 5. The scenarios included considering the confidence values of $z_{pt} = 0.5$ (NC), $z_G = 0.6$ (Global), and a separate z_{pt} for each task (PerTask). The results indicate that, in the 1st and 20th tasks about 100% of the input queries were classified as *Easy* in all the scenarios, while in the worst case, less than 2% of the input queries of the 2nd task were determined as *Easy* input queries in different scenarios. The last three bars in this figure show the average percentages of the *Easy* input queries among all the tasks (denoted as Avg) in all the three considered scenarios. It reveals that 75% of the inputs were considered as *Easy* ones when the activation module was not employed (the NC scenario), while 67% (63%) of the inputs were detected as *Easy* in the Global (PerTask) scenario. Also, the ratio of the inputs that classified as *Easy* decreased when the activation module was employed. This originated from the fact that the false positive (negative) classifications were reduced (increased) in the Global and PerTask scenarios. Figure 6 depicts the accuracy of ICN for the three scenarios based on considered confidence threshold values. The results reveal that considering these confidence threshold values leads to the overall accuracy reduction of ICN (due to more

false negative inputs). Also, it is evident that in the case of the PerTask scenario, the accuracy decrease for ICN is more than the Global scenario. This is due to the use of the activation module for reducing the false positive (FP) metric of ICN which leads to the accuracy improvement of A²P-MANN. The results suggest that the FP metric of ICN in PerTask scenario be the lowest among the three scenarios. Table 3 contains the minimum, maximum, and average false positive and false negative (FN) metrics of the ICN network for the scenarios. The results show that the FN of the proposed ICN is larger than its FP (on average, by $\sim 4\times$). Apparently, FN does not impact the final accuracy of the A²P-MANN. The FP of the ICN when the activation module is employed was reduced. As was expected, the lowest FP belonged to the PerTask scenario. The accuracy of ICN (without considering the confidence threshold) was about 100% in the case of the 1st and 20th tasks while the lowest one belonged to the 3rd task with the accuracy of 66%. On average, the accuracy of ICN was 86%, 81%, 79% in the cases of NC, global, and PerTask scenarios, respectively.

Finally, the A²P-MANN accuracy is compared to that of the baseline MANN under the Global and PerTask scenarios. The results of this comparison which are plotted in Fig. 7, demonstrate that, in the worst case, a 4.6% accuracy loss in task 14 was yielded, while in some cases (e.g., tasks 11 and 13) the accuracy was improved up to 2.7%. As stated before, the considered parameters for the pruning techniques (as well as Zero-Skipping) had no adverse effect on the accuracy. This implies that the degradation should be attributed to the input classifier network and FC_E efficiency.

It should be noted that considering different confidence values for the tasks (the PerTask scenario) results in a higher accuracy for A²P-MANN compared to the Global scenario. In the PerTask scenario, the accuracy loss was limited to 1% for each task. On average, the PerTask (Global) scenario led to 0.1% (1%) A²P-MANN accuracy loss compared to that of the baseline MANN.

Platform Independent Performance Evaluation: To determine the performance improvement of A²P-MANN (with and without using the zero-skipping technique [16]) compared to the baseline MANN for Pre-Embedded and Interactive application types, we have utilized (5)-(7). Figure 8 shows the flops reductions (performance improvement) of A²P-MANN in different tasks of bAbI in the Global and PerTask scenarios. Also, in this figure, the reductions due to using the zero-skipping technique for the baseline MANN are provided. The parameter θ_{ZS} was considered as 0.01,

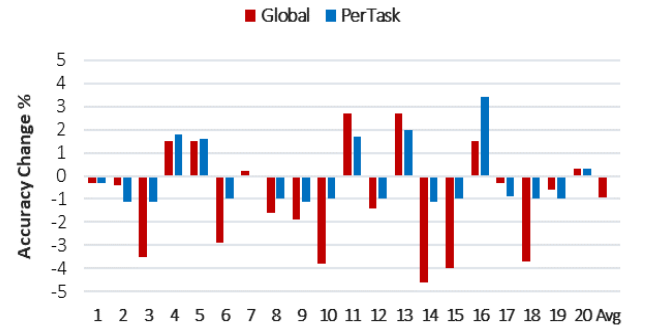


Figure 7. Accuracy loss of A²P-MANN compared to the baseline MANN under two considered scenarios.

providing an 81% overall reduction in the weighted sum operations without any accuracy loss [16]. More precisely, our results indicated that 40% (23%) of the achieved reduction in the Interactive (Pre-Embedded) application type was due to the zero-skipping technique. On the other hand, the A²P-MANN inference reached, on average, 45.6% (44.8%) and 44.2% (42.5%) reductions for all the tasks in the Pre-Embedded (Interactive) application type in the Global and PerTask scenarios compared to the baseline network, respectively. When the zero-skipping technique was used in the A²P-MANN inference process, an overall of 68% (59%) and 66% (57.5%) computation reductions for Interactive (Pre-Embedded), in the Global and PerTask scenarios, respectively, were achieved.

Platform Dependent Performance Evaluation: To compare the performance (*i.e.*, latency) of A²P-MANN to that of the baseline MANN, we implemented them using PyTorch and executed them on the CPU (Intel Core i7-4790) and GPU (Nvidia 1080ti with 12GB memory). In this study, due to the similarity between the performance of the Global and PerTask scenarios, only the global confidence threshold was included. Due to the small value of number of sentences in each story, n_s , (*i.e.*, 50) of the baseline network, the accurate execution time measurement was not possible. Thus, we have enlarged the n_s of the considered network to 50K (5K) for the Pre-Embedded (Interactive) cases. A similar approach of enlarging the dataset by assuming an n_s of 100M for showing the capability of the zero-skipping algorithm in reducing the runtime of MANN was used in [16]. Also, the zero-skipping technique was not used in the platform dependent study because of its ineffectiveness (and also even harmful) in some cases (especially, on GPUs) [16].

The normalized latencies of A²P-MANN with respect to the baseline MANN on CPU and GPU platforms are illustrated in Fig. 9. As the figures indicate, on CPU, on average, a 40% (43%) latency reduction compared to the baseline MANN for Pre-Embedded (Interactive) application

types for the A²P-MANN inference is achieved. On GPU, our proposed inference technique led to a 33% (41%) latency reduction, on average, compared to that of the baseline network for Pre-Embedded (Interactive). Due to the large considered n_s , most of the overall computations belonged to the attention inference hops, and thus, most of the achieved latency reductions were owing to the utilization of ICN while the effect of the pruning techniques was negligible. For the 1st and 20th tasks, which had the maximum number of *Easy* inputs, the highest latency reductions of ~63% on CPU and 52% and 62% on GPU for Pre-Embedded and Interactive applications, respectively, were obtained. On the other hand, because of very few numbers of *Easy* input queries in the 2nd and 3rd tasks, the overhead of the ICN was large lowering the gain of the low computations of *Easy* inputs.

Finally, it should be mentioned that we used a smaller number of sentences for the Interactive applications in the study owing to the fact that the database should be provided by the user in this case (*e.g.*, the contents of a book that the user has read, as stated in [16]). Obviously, embedding more sentences needs more time and energy. Thus, this limits the usage of the interactive approach for large databases. Nevertheless, to show the effectiveness of the proposed inference approach for large interactive applications, we repeated the study for $n_s = 50K$. The obtained timing results show, on average, about 44% latency reduction when using A²P-MANN. The reduction is larger than the values reported for the smaller databases.

VI. CONCLUSION

In this paper, we proposed A²P-MANN which was a computationally efficient inference method. It dynamically controlled the number of required hops in a memory-augmented neural network. In its structure, a small additional input classifier network after the first hop determined whether the input is easy or hard. For easy inputs, the answer was extracted after the first hop using a retrained

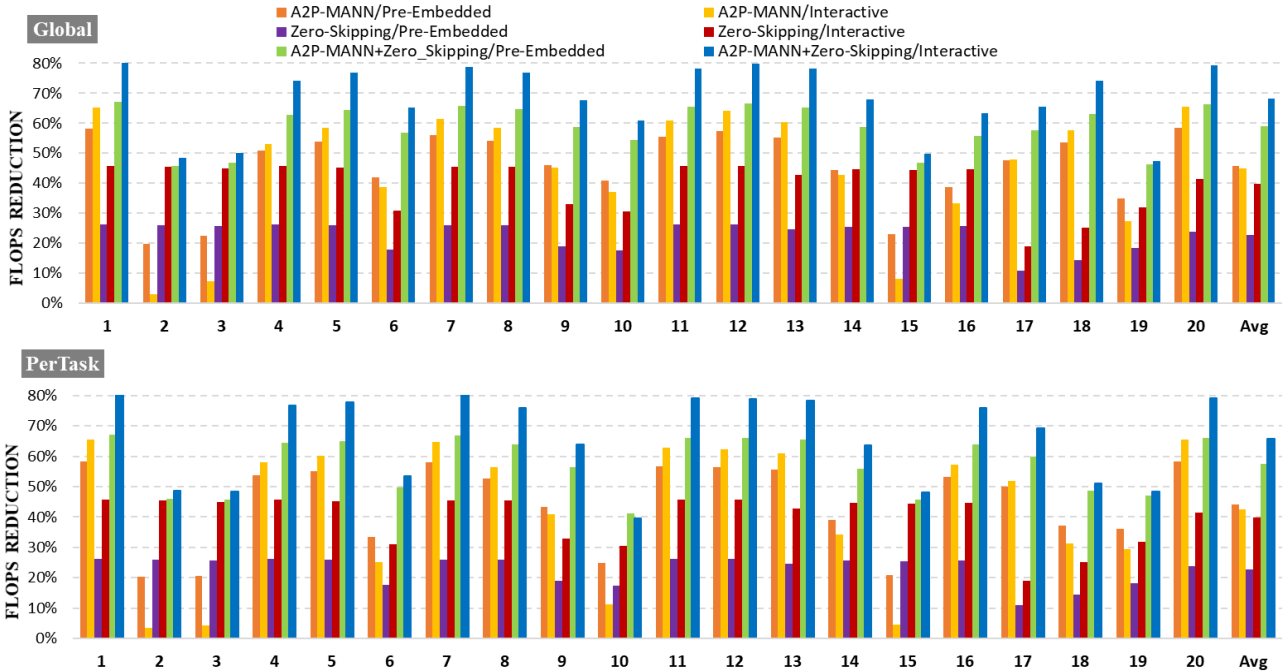


Figure 8. Computation reduction on 20 tasks of bAbI dataset using A²P-MANN inference (and zero-skipping) under Global and PerTask scenarios.

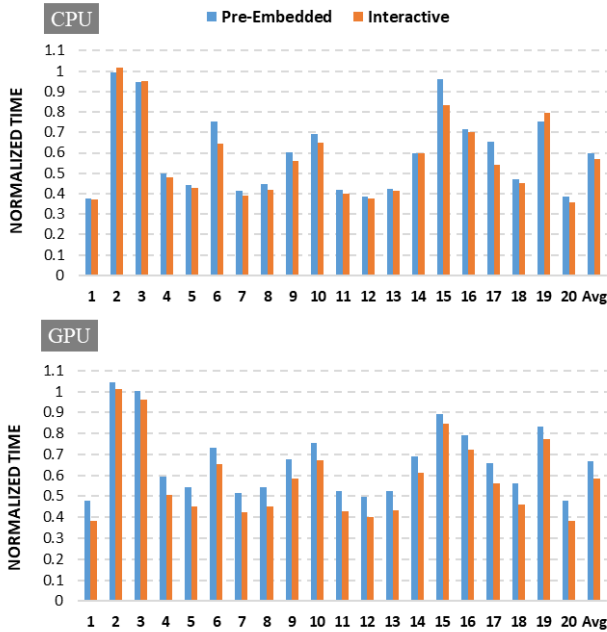


Figure 9. The normalized latency of A²P-MANN inference with respect to the baseline MANN on the CPU and GPU platforms.

FC layer. For hard inputs, the calculations of remaining hops before using the final FC layer were performed. Also, to further reduce the computation in A²P-MANN, two methods for pruning the weight matrices of the FC layers were proposed. In the first one, *unused* rows of the final weight matrices found by analyzing the training labels were eliminated during inference. The second pruning method found *unimportant* rows by counting the number of small weights in each row. The suggested computation reduction techniques were independent from the hardware platform. The proposed approach was particularly suitable for resource-constrained environments such as embedded systems. The results obtained in this work showed about 42% computation reduction at the cost of less than 1% accuracy loss, on average, for A²P-MANN when compared to the baseline MANN. Also, combined with zero-skipping, A²P-MANN achieved more than 57% (up to 68%) of computation reduction. Finally, it resulted in more than 40% latency reduction on a CPU while an average latency reduction of more than 33% (41% for interactive use cases) was achieved on a GPU.

REFERENCES

- [1] V. Sze, Y. H. Chen, T. J. Yang, and J. S. Emer, "Efficient Processing of Deep Neural Networks: A Tutorial and Survey," *Proceedings of the IEEE*, vol. 105, no. 12, Institute of Electrical and Electronics Engineers Inc., pp. 2295–2329, Dec. 01, 2017, doi: 10.1109/JPROC.2017.2761740.
- [2] S. Han, H. Mao, and W. J. Dally, "Deep Compression: Compressing Deep Neural Networks with Pruning, Trained Quantization and Huffman Coding," *4th Int. Conf. Learn. Represent. ICLR 2016 - Conf. Track Proc.*, Oct. 2015, [Online]. Available: <https://arxiv.org/abs/1510.00149v5>.
- [3] T.-J. Yang, Y.-H. Chen, and V. Sze, "Designing energy-efficient convolutional neural networks using energy-aware pruning," in *Proceedings of the IEEE Conference on Computer Vision and Pattern Recognition*, 2017, pp. 5687–5695.
- [4] S. Han, J. Pool, J. Tran and W. Dally, "Learning both weights and connections for efficient neural network," in *Proc. Adv. Neural Inf. Process. Syst. (NIPS)*, vol. 28, pp. 1135–1143, 2015.
- [5] E. Park *et al.*, "Big/little deep neural network for ultra low power inference," in *2015 International Conference on Hardware/Software Codesign and System Synthesis (CODES+ISSS)*, Oct. 2015, pp. 124–132, doi: 10.1109/CODES+ISSS.2015.7331375.
- [6] H. Tann, S. Hashemi, R. I. Bahar, and S. Reda, "Runtime configurable deep neural networks for energy-accuracy trade-off," in *2016 International Conference on Hardware/Software Codesign and System Synthesis (CODES+ISSS)*, Oct. 2016, pp. 1–10.
- [7] S. Venkataramani, A. Ranjan, K. Roy, and A. Raghunathan, "AxNN: Energy-efficient neuromorphic systems using approximate computing," in *2014 IEEE/ACM International Symposium on Low Power Electronics and Design (ISLPED)*, Aug. 2014, pp. 27–32, doi: 10.1145/2627369.2627613.
- [8] S. Sukhbaatar, A. Szlam, J. Weston and R. Fergus, "End-to-end memory networks," in *Proc. Adv. Neural Inf. Process. Syst. (NIPS)*, pp. 2440–2448, 2015.
- [9] J. Weston, S. Chopra, and A. Bordes, "Memory Networks," *3rd Int. Conf. Learn. Represent. ICLR 2015 - Conf. Track Proc.*, Oct. 2014.
- [10] A. Graves, G. Wayne, and I. Danihelka, "Neural Turing Machines," Oct. 2014, arXiv:1410.5401. [Online]. Available: <http://arxiv.org/abs/1410.5401>.
- [11] A. Graves *et al.*, "Hybrid computing using a neural network with dynamic external memory," *Nature*, vol. 538, no. 7626, pp. 471–476, Oct. 2016, doi: 10.1038/nature20101.
- [12] Y. LeCun, "1.1 Deep Learning Hardware: Past, Present, and Future," in *2019 IEEE International Solid-State Circuits Conference - (ISSCC)*, Feb. 2019, vol. 2019-Febru, pp. 12–19, doi: 10.1109/ISSCC.2019.8662396.
- [13] J. Dodge *et al.*, "Evaluating Prerequisite Qualities for Learning End-to-End Dialog Systems," *4th Int. Conf. Learn. Represent. ICLR 2016 - Conf. Track Proc.*, Nov. 2015.
- [14] F. Hill, A. Bordes, S. Chopra, and J. Weston, "The Goldilocks principle: Reading children's books with explicit memory representations," Nov. 2016, arXiv: 1511.02301. [Online]. Available: <http://arxiv.org/abs/1511.02301>.
- [15] J. E. Weston, "Dialog-based language learning," in *Proc. Adv. Neural Inf. Process. Syst. (NIPS)*, pp. 829–837, Apr. 2016.
- [16] H. Jang, J. Kim, J.-E. Jo, J. Lee, and J. Kim, "MnnFast: A Fast and Scalable System Architecture for Memory-augmented Neural Networks," in *Proceedings of the 46th International Symposium on Computer Architecture*, Jun. 2019, pp. 250–263, doi: 10.1145/3307650.3322214.
- [17] J. R. Stevens, A. Ranjan, D. Das, B. Kaul, and A. Raghunathan, "Manna: An accelerator for memory-augmented neural networks," in *Proceedings of the 52nd Annual IEEE/ACM International Symposium on Microarchitecture*, Oct. 2019, pp. 794–806, doi: 10.1145/3352460.3358304.
- [18] S. Park, J. Jang, S. Kim, and S. Yoon, "Energy-Efficient Inference Accelerator for Memory-Augmented Neural Networks on an FPGA," in *2019 Design, Automation & Test in Europe Conference & Exhibition (DATE)*, Mar. 2019, pp. 1587–1590, doi: 10.23919/DATE.2019.8715013.
- [19] J. Weston *et al.*, "Towards AI-Complete Question Answering: A Set of Prerequisite Toy Tasks," *4th Int. Conf. Learn. Represent. ICLR 2016 - Conf. Track Proc.*, Feb. 2015.
- [20] O. Temam, "A defect-tolerant accelerator for emerging high-performance applications," in *2012 39th Annual International Symposium on Computer Architecture (ISCA)*, Jun. 2012, pp. 356–367, doi: 10.1109/ISCA.2012.6237031.
- [21] C. Torres-Huitzil and B. Girau, "Fault and Error Tolerance in Neural Networks: A Review," *IEEE Access*, vol. 5, pp. 17322–17341, 2017, doi: 10.1109/ACCESS.2017.2742698.
- [22] T.-W. Chin, C. Zhang, and D. Marculescu, "Layer-compensated Pruning for Resource-constrained Convolutional Neural Networks," Sep. 2018, arXiv: 1810.00518. [Online]. Available: <http://arxiv.org/abs/1810.00518>.
- [23] G. Gobieski, B. Lucia, and N. Beckmann, "Intelligence Beyond the Edge," in *Proceedings of the Twenty-Fourth International Conference on Architectural Support for Programming Languages and Operating Systems*, Apr. 2019, pp. 199–213, doi: 10.1145/3297858.3304011.
- [24] B. Reagen *et al.*, "Ares: A framework for quantifying the resilience of deep neural networks," in *2018 55th ACM/ESDA/IEEE Design Automation Conference (DAC)*, Jun. 2018, pp. 1–6, doi: 10.1109/DAC.2018.8465834.

- [25] M. Ali, A. Agrawal, and K. Roy, "RAMANN: In-SRAM Differentiable Memory Computations for Memory-Augmented Neural Networks," in *Proceedings of the ACM/IEEE International Symposium on Low Power Electronics and Design*, Aug. 2020, pp. 61–66, doi: 10.1145/3370748.3406574.
- [26] G. Huang, D. Chen, T. Li, F. Wu, L. van der Maaten, and K. Q. Weinberger, "Multi-Scale Dense Networks for Resource Efficient Image Classification," Mar. 2017, arXiv: 1703.09844. [Online]. Available: <http://arxiv.org/abs/1703.09844>.
- [27] P. Panda, A. Sengupta, and K. Roy, "Energy-Efficient and Improved Image Recognition with Conditional Deep Learning," *ACM J. Emerg. Technol. Comput. Syst.*, vol. 13, no. 3, pp. 1–21, May 2017, doi: 10.1145/3007192.
- [28] O. Press and L. Wolf, "Using the Output Embedding to Improve Language Models," *15th Conf. Eur. Chapter Assoc. Comput. Linguist. EACL 2017 - Proc. Conf.*, vol. 2, pp. 157–163, Aug. 2016, [Online]. Available: <http://arxiv.org/abs/1608.05859>.
- [29] J. Perez and F. Liu, "Gated End-to-End Memory Networks," *15th Conf. Eur. Chapter Assoc. Comput. Linguist. EACL 2017 - Proc. Conf.*, vol. 1, pp. 1–10, Oct. 2016.
- [30] H. A. Thant, Khaing Moe San, Khin Mar Lar Tun, T. T. Naing, and N. Thein, "Mobile Agents Based Load Balancing Method for Parallel Applications," in *6th Asia-Pacific Symposium on Information and Telecommunication Technologies*, Nov. 2005, pp. 77–82, doi: 10.1109/APSITT.2005.203634.
- [31] <https://github.com/domluna/memnn2n>.
- [32] A. Paszke *et al.*, "PyTorch: An Imperative Style, High-Performance Deep Learning Library," in *Proc. Adv. Neural Inf. Process. Syst. (NIPS)*, 2019, vol. 32, pp. 8026–8037.